A Frequency Metrology approach to Newtonian constant *G* determination using a pair of extremely high *Q* simple pendulums in free decay

A De Marchi
Dept. of Electronics and Telecommunications, Politecnico di Torino, Torino, Italy
E-mail: andrea.demarchi@polito.it

Abstract. It is argued that simple pendulums exhibiting *Q* values in excess of 10^8 can be realized by using high strength fibres to suspend in vacuum a bob of less than 10^{-3} kg. For a 1 m long pendulum this means damping time constants of several years, long enough to allow experiments in free decay mode, maximizing in this way the expected short term frequency stability. A dual pendulum experiment based on this projection is discussed, which common-modes seismic noise and is expected to yield 10^{-5} uncertainty on Big G. The value of the latter can be obtained from the variation in relative frequency difference between the two pendulums when they are subjected to well controlled variations of the gravitational field. A discussion is given of Type A and Type B uncertainty contributions, and a tentative accuracy budget is projected.

1. Introduction

The measurement of the Newtonian constant *G* is difficult for the feebleness of the gravitational force both absolute and relative to other forces associated with different phenomena, in the presence of which experiments aimed at measuring *G* must be carried out. This poses two orders of problems which are typically in competition, as both A and B Type uncertainties must be reduced below the desired level. On one hand, in fact, the need to avoid too low S/N ratios suggests privileging experimental designs yielding as great a signal as possible, even if it implies accepting hard to model features, putting in this way a stress on Type B uncertainty; on the other hand the choice of an approach which can be very well modeled often pays a tribute to S/N ratio, putting a stress on Type A uncertainty. It is no wonder that all efforts to measure *G* were undertaken with an S/N ratio maximizing approach, in an era when the high resolution now possible in measurements was unthinkable. However, a re-visitation of this trade-off is here suggested, at the light of contemporary amazing Time and Frequency Metrology resolutions. It is claimed that it may offset toward the latter end of the scale the positioning of the best approach choice.

As a matter of fact, while all ten evaluations of *G* reported in the 19th century, all four made in the first half of the 20th century (only one of which was claimed to have an accuracy better than 0.1%), and all those published after WWII and before 1990 by half a dozen groups, all were obtained with basically the same approach adopted by Henry Cavendish more than two centuries ago [1], substantially different experiments started to crop up thereafter.

Three facts concurred in steering the quest for *G* into new ways: theoretical doubts raising in the mid-80s on the validity of the Newtonian theory (the fifth force debate), a result with a discrepancy of many standard deviations from the accepted value which was published by a highly respected institution [2], and the discovery by Kuroda [3] of a possible source of error in Cavendish balances, hidden in the an-elasticity of the torsion wire.

As a result, at least a dozen different evaluations have been carried out in as many different groups in the last twenty years, a number of which have adopted a totally different approach from the torsion balance, using as a sensitive device either a beam (Jolly-Poynting) balance, or a free-fall gravimeter, or a simple pendulum, all avoiding in one way or another the torsion wire problem.

In the best experiment with the **beam balance**, carried out in Zurich [4], 1 kg test masses sat on either dish and 4 ton of Mercury were moved up above and down below one of the two. The 1.8×10^{-5} final uncertainty claimed by the group is one of the best to date. A great deal of beautiful error analysis and correction was carried out in this high sensitivity experiment.

The **free-fall gravimeter** is blessed by the absence of suspensions, but no uncertainties better than 10^{-3} have yet been claimed as relative resolution is a problem. In fact, the measured gravitational force is compared directly to the attraction by the whole Earth. Despite the adoption of laser interferometry in one case [5], and atom interferometry in two more [6,7], requirements are so great that measurements remained limited in all cases by Type A uncertainty even after long averages. The positioning of the free-fall approach in the range of possible choices seems to be too biased toward error reduction at all cost, even for modern high resolution measurement technology, because the effect vanishes exactly where one would like to have it most strong, at the center of the active masses.

The **simple pendulum** approach was used in three experiments, two of which in the static mode. In both, two hanging test masses held Fabry-Perot mirrors whose spacing changed as an effect of active masses displacement. The measured quantity was the resonant frequency. In one case the latter was in the microwave range [8] and an accuracy slightly better than 10^{-3} was claimed, in the other it was in the visible [9] and the claimed accuracy was in the low 10^{-5} range. The third attempt, which employed a **dynamic pendulum** approach, is the small scale pilot experiment which was carried out at Politecnico di Torino [10] from 1998 to 2005. This preliminary trial yielded an evaluation of G with a seismic noise limited Type A uncertainty of 3%, nevertheless providing critical indications for this new proposal. Relevant for the accuracy of this and any dynamic experiment is the analysis, carried out within this work, of the frequency change that is induced by variations of the energy stored in the oscillations when the active masses are moved [11]. This approach can be viewed as using a "constrained free-fall", which positions it less far out than the true free-fall toward the same end of the scale. In fact, the signal force is here compared to only a component of Earth's attraction, which also vanishes at rest position. This maximizes the effect exactly where desired, contrary to the free-fall case, as argued in section 3.

In truth, some of the best results ever published to date, with uncertainties in the mid to low 10^{-5} range, have been obtained in this post-Kuroda era with some variation of the **torsion balance**, including both static mode and dynamic mode operation. Two of these were obtained in the static mode, and claimed uncertainty of $1.38 \cdot 10^{-5}$ [12] and $4.05 \cdot 10^{-5}$ [13] respectively by avoiding altogether any torsion in the wire with the help of a feedback system that forced the moving apparatus to stay put. Similar accuracy was also claimed by a group at BIPM [14], where a strip was used for a torsion wire, in order to reduce shear strains in deflection, and the residual an-elasticity Kuroda effect was evaluated in dynamic mode operation. In another group, the an-elasticity of the torsion wire was measured separately [15], to evaluate the correction to be made in a dynamic mode measurement.

Unfortunately, in spite of progress made both with the traditional torsion balance approach and with other methods, significant discrepancies persist among different evaluations, which makes the CODATA Group cautious in citing uncertainty. At present, in the most recent CODATA 2014 revision, the relative uncertainty is indicated to be $4.7 \cdot 10^{-5}$ on a value of $6.67408 \cdot 10^{-11}$ $m^3kg^{-1}s^{-2}$.

In recognition of the basic metrological principle that the only way to mitigate the risk of embarking unknown systematics in the assessment of a natural object is to obtain compatible results with many totally independent approaches (Karl Popper teaching here!), the present proposal is aimed at reaching the ultimate potential of the dynamic pendulum approach by overcoming with typical Time and Frequency Metrology methods the limitations of the pilot experiment.

A dual pendulum configuration is proposed, aimed at exploiting the fast reduction of statistical uncertainty granted by measuring the variation rate of time delay between the two, which is well known to be equal to their relative frequency difference [16], and at the same time common-moding the relevant 0.2 Hz seismic angular noise due to ocean waves excited Rayleigh waves [10,17] which disturbed period measurement in the pilot experiment. The inferred possibility of reaching pendulum Q values in excess of 10^8 enables free decay operation for months, high frequency stability, and the projection of 10^{-5} uncertainty on G in a few weeks of data taking.

In section 2 the critical point of such high Q values possibility is addressed, as it has direct impact on design, and in section 3 the plan of the experiment is described. In section 4 the projected accuracy budget is presented and shortly discussed, with an indication of expected future improvements.

2. *Q* analysis

To be sure, a well-known truism is that a high Q factor is fundamental for both Type A and Type B uncertainties in an experiment involving an excited resonator, because it generally fosters high short term frequency stability and guarantees for the ability to closely model it. In the torsion balance, for example, a high Q can be taken as a proof of low torsion wire an-elasticity and support high accuracy claims in the analysis of the Kuroda effect, as in the case of the BIPM experiment, which featured a Q of 10^5, the best ever reported in torsion balances for big G determinations.

However, further specific reasons to seek as high a Q as possible in this dual dynamic pendulum configuration include noise filtering action, the need to avoid frequency locking of the two pendulums, and the beauty of long ring-down time constant. In particular, the latter can be as long as several years for a 1m long pendulum with Q in the mid-10^8 range, which would enable a several months long experiment in free decay mode, avoiding both the risk of noise injection with the sustainment mechanism and the frequency drift deriving from the coupling of period and amplitude if the latter is not constant.

Apart from friction on residual air, which however can be reduced below any desired level with adequate vacuum, only two main loss mechanisms were identified in a fibre pendulum realized as pictured in figure 1: the cyclic stretching of the fibre under the action of varying centrifugal force and gravity component along the fibre, and the cyclic bending of the fibre as it wraps and unwraps onto the suspension profile. The latter is assumed circular in figure 1 for ease of implementation reasons, and because a circular profile turns out to produce a minimum at non-zero amplitude in the period versus swing angle curve, which can be exploited to make the pendulum locally isochronous [18].

A first approximation theory can be developed for the contributions of these two mechanisms to pendulum Q by overlooking the cyclic length variations. Expressions for Q_s (stretching) and Q_b (bending) can be rather easily obtained with this simplification, and then combined to predict Q as

$$\frac{1}{Q} = \frac{P_{ds}+P_{db}}{\omega_p E_p} = \frac{1}{Q_s} + \frac{1}{Q_b} \quad , \tag{1}$$

where the index p of resonance angular frequency ω_p and of energy E_p stored in the oscillation indicates that they are relative to the pendulum mode, and dissipated power P_d of the two mechanisms is identified by the second index s or b. Such power can be written for both as a function of pendulum frequency and energy, as in equation (1), but also as a function of eigen-frequency and stored energy of the mode that sustains either loss mechanism, i.e. the stretching and the bending mode. In this latter case the Q value that must be used in the formula is the intrinsic value Q_f of the fibre material, which can in principle be measured by exciting the relevant stretching or bending mode. In practice, this can be easily done on Earth only for the stretching mode because selectively exciting the bending mode to measure frequency and Q would require a gravity free experiment. So it is

$$P_{ds} = \frac{\omega_p E_p}{Q_s} = \frac{\omega_s E_s}{Q_f} \quad , \tag{2}$$

$$P_{db} = \frac{\omega_p E_p}{Q_b} = \frac{\omega_b E_b}{Q_f} \, . \tag{3}$$

Notice that E_s and E_b represent the energy stored in the stretching and bending modes when they are excited out of frequency at the natural pendulum resonance ω_p and at the actual swing amplitude θ_0.

Now, for the stretching mode, it turns out that the energy E_s stored in it, swapping at double the pendulum frequency between elastic and kinetic energy, is related to pendulum energy by

$$\frac{E_p}{E_s} = \frac{16}{9\theta_0^2 \varepsilon_0} \quad , \tag{4}$$

where ε_0 is the static strain, and the ratio between pendulum and stretching mode frequency is easily seen to be

$$\frac{\omega_p}{\omega_s} = \sqrt{\varepsilon_0} \quad , \tag{5}$$

so that, by combining equations (2), (4) and (5), the following expression is obtained for the contribution to pendulum Q from the stretching mode

$$\frac{Q_s}{Q_f} = \frac{16}{9\theta_0^2\sqrt{\varepsilon_0}} \quad . \tag{6}$$

Similarly, for the bending mode, ratios relating energy E_b stored in it to pendulum energy, and its natural frequency to pendulum frequency, can be shown to be

$$\frac{E_p}{E_b} = \left(\frac{\omega_p}{\omega_b}\right)^2 = \frac{LD_b}{D_f^2}\varepsilon_0\theta_0 \quad . \tag{7}$$

The frequency ratio can be derived easily by equating the peak potential elastic energy stored in the fibers to the peak kinetic energy calculated in the sine wave approximation. The contribution to pendulum Q from the bending mode can then be calculated by combining equations (3) and (7), and is

$$\frac{Q_b}{Q_f} = \left(\frac{LD_b}{D_f^2}\varepsilon_0\theta_0\right)^{3/2}. \tag{8}$$

The combination of these two contributions leads to the values shown in figure 2 for the total Q of the pendulum as a function of oscillation amplitude θ_0 in various configurations of circular suspension diameter and fibre type. It is here assumed that the mass of the bob be 0.16 g, which was the mass of the 5 mm BK7 ball lens used in the pilot experiment, for which the lowest curve holds.

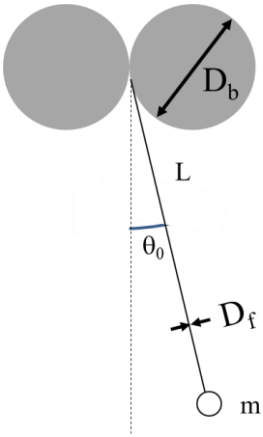

Figure 1. Pendulum configuration and parameters definition. Circular suspension profiles were chosen for ease of precise implementation and coherence between design and theory.

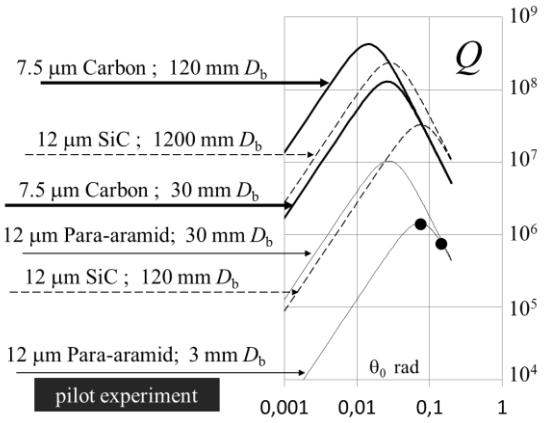

Figure 2. Pendulum Q values calculated for various fibres and suspension diameters. The two dots are measured Q for the pilot experiment. Their agreement with the theory supports its validity, and the confidence that it may be extrapolated to different configurations.

The selection of suitable fibres is mainly guided by equations (6) and (8), summarized in figure 2, which suggest looking through thin high stiffness fibres for Q maximization. However, it must be pointed out here that characterization of mechanical losses in such high strength fibres is typically not to be found in the technical literature. The intrinsic Q of candidate fibre materials was therefore measured in order to produce the results reported in figure 2. This was done by evaluating the Q of a spring-mass resonator in which the spring was a bundle of a reasonably well known number of fibres. Q_f values of 120, 470, and 1000 were found for Para-aramidic, SiC, and Carbon fibres respectively [19].

Clearly, the pendulum configuration should be designed for maximum Q at the desired oscillation amplitude, which in turn must be decided in considering issues like a good match with minimization of period and ease of correlation between measured frequency departure and gravitational effect.

3. Planning the experiment

The experiment which is being implemented includes two 1 m long pendulums oscillating in the same plane about 100 mm apart, and an ensemble of cylindrical Tungsten masses laying either side of such plane, outside the vacuum container, with a small separation in between, where the bob swings inside the container. The bob is a 5 mm diameter BK7 ball lens suspended by two converging fibres which wrap and unwrap on two cylindrical profiles as depicted in figure 1. The arrangement removes the degeneracy with the transversal mode and obliterates undesired Coriolis effects. Active masses are moved periodically back and forth in the two configurations of figure 3, alternately with one pendulum swinging between two pairs of masses and the other in the gap for half the repetition period T_R and vice-versa for the other half. Half the calculated acceleration a_M added by the active masses system, divided by the acceleration due to Earth's gravity a_g, is shown in figure 4 versus pendulum distance from system center. More details are given below, where the near equality between such half ratio and the relative frequency shift is discussed. If perfect equivalence between the two is assumed for the time being, the difference between the two relative frequency differences is twice the sum of a_M/a_g for both pendulums.

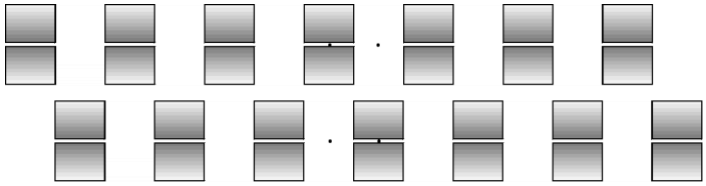

Figure 3. Scheme of the two configurations of active masses. Rest positions of the two bobs are shown by black dots. Subtracting the relative frequency differences in the two configurations doubles the sum of both relative shifts.

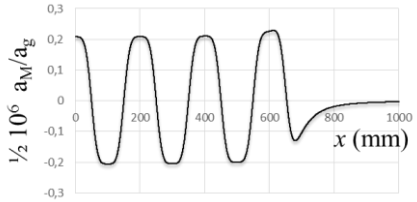

Figure 4. Relative extra acceleration versus distance from center for the Tungsten masses of figure 3. Frequency shifts are roughly equal to ½ a_M/a_g.

In either configuration the time delay rate of change between the two pendulums is measured with two optical high resolution Position Sensitive Detectors (PSD) at the bobs' rest points [10], which in principle yields their relative frequency difference in the most precise measurement of any quantity made available by modern Metrology [16]. This fact, together with the common-moding of angular seismic noise that the dual pendulum solution can provide, makes of this proposed scheme a totally new experiment, and not "just an incremental improvement" on the pilot experiment any more than most *G* determinations have been with respect to the original Cavendish experiment.

A slight mistuning must be imposed between the two pendulums to keep signal injection induced frequency pulling low, but this is really easy given the high projected *Q* values for the pendulums. In fact, even at high coupling (e.g. 10^{-2}) a relative mistuning of 10^{-8} is more than adequate [20,21] to keep pulling below the 10^{-12} level that would start to be relevant for the target 10^{-5} accuracy. It would be hard to avoid such mistuning, but at any rate a rational frequency ratio $(n\text{-}1)/n$ is here planned between the two, in order to get them back in phase every *n* periods, and design the period of such occurrence.

Delay data will be taken at such times in order to guarantee adequate Common Mode Rejection (CMR) of the angular seismic noise that introduced on the single period measurement a white noise level of the order of 3 μs in the pilot experiment. It must be pointed out here for clarity that angle noise in the oscillation plane is not filtered by the pendulum *Q*, as it amounts to a rotation of the laboratory. As ocean waves excited angular noise at 0.2 Hz is sampled at pendulum frequency, such angle noise comes by aliasing to be white delay time noise. Regression on *N* delays will then improve it by $N^{-1/2}$, and division by *NT* to get the slope will yield a relative frequency resolution $\sigma_y(\tau)$ that improves as $N^{-3/2}$ upon averaging *N* results [16]. If the necessary 2 to $3\cdot10^{-12}$ Type A uncertainty is desired in 10^4 s (about 2.5 hours, or 250 measurements of 40 s), the single shot $\sigma_y(\tau)$ should then be about 10^{-8}, which places at $4\cdot10^{-7}$ the needed single differential delay uncertainty (≈300 ns on single delay). This represents a factor of 10 CMR of angular seismic noise at 0.2 Hz. Such noise should in principle be sampled at the same instant for the two pendulums in order to be perfectly rejected, and the maximum time delay between the two that is acceptable for the desired rejection must be studied.

So, while the *rms* period uncertainty $\delta T_{\rm rms}$ produced in the pilot experiment by the Rayleigh-waves quasi-coherent angle noise of *rms* value $\delta\theta_{\rm rms}$ was

$$\delta T_{rms} = \frac{\sqrt{2}}{\omega_p}\frac{\delta\theta_{rms}}{\theta_0} \quad , \tag{9}$$

the *rms* delay uncertainty $\delta(\Delta t)_{\rm rms}$ produced in this experiment by the same angle noise, if the measured delay is Δt, can be easily shown to be

$$\delta(\Delta t)_{rms} = \Delta t\,\frac{\omega_R}{\omega_p}\frac{\delta\theta_{rms}}{\theta_0} \tag{10}$$

when calculated from the time derivative of the quasi-sine-wave angular noise at the frequency $\omega_{\rm R}$ of Rayleigh waves. From the ratio of equations (9) and (10), the maximum delay can be calculated at which a given minimum CMR of the bright angular seismic noise spectral line is obtained in the dual pendulum configuration. For equal amplitude θ_0 in the two experiments, the constraint is

$$\Delta t < \frac{\sqrt{2}}{CMR\;\omega_R} \quad . \tag{11}$$

For the actual frequency of Rayleigh waves and the desired CMR, equation (11) indicates 100 ms as the maximum acceptable delay. This is the reason why a rational (n-1)/n frequency ratio is designed for the two pendulums, so that every n periods they be in phase at the detector location. On the other hand, since every period the slower pendulum's delay increases by about T/n, the minimum value of n that guarantees at least one delay measurement of less than 100 ms at that time is 20, because the pendulum period is about 2 s. The choice of n=21 is proposed here only for discussion purposes. Greater values would offer more useable delay data per coincidence but increase their distance in time.

The relevant time delay slope s is indicated in figure 5 in the delay-versus-time space. Instrumental resolution is clearly not a problem for a desired delay uncertainty of 300 ns, nor is a particularly accurate reference frequency necessary of the time interval counter.

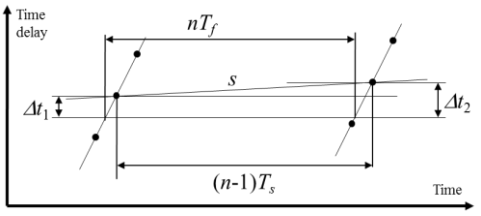

Figure 5. Measured time delay rate (slope s). Dots are ticks from the slow pendulum.

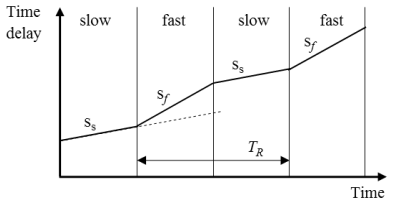

Figure 6. Delay slope changes as active masses are moved from slow to fast pendulum and back.

In figure 6, a picture is given of how time delay slope is expected to change when the center of the active masses system is moved back and forth between left and right pendulums. The relevant information for the extraction of a G value is the difference $\Delta s = s_f - s_s$ between the slopes measured with active masses centered on the fast pendulum and the slow one. In fact, it can be easily shown that Δs is directly proportional to the average of relative frequency shifts y_{Mf} and y_{Ms} induced by active masses on fast and slow pendulum respectively. With slopes calculated as $(\Delta t_2 - \Delta t_1)/(nT_f)$, the slope difference is

$$\Delta \boldsymbol{s} = \frac{\boldsymbol{n-1}}{\boldsymbol{n}}\frac{\boldsymbol{T_s}}{\boldsymbol{T_f}}\boldsymbol{2}\left(\boldsymbol{y_{Mf}} + \boldsymbol{y_{Ms}}\right), \tag{12}$$

where the ratios T_s/T_f and (n-1)/n were not simplified because in the actual experimental arrangement they may not exactly compensate as they should.

As for the calculation of the gravitational effect on frequency, the relative extra acceleration given to the bob by the active masses system is the relevant parameter because, inasmuch as the oscillation of the bob's displacement x is a sine wave, by the second law of dynamics its angular frequency is given by $\omega_M^2 = (a_g + a_M)/x$, with $a_g = gx/L$ and ω_M the angular frequency as modified by the active masses.

Both a_g and a_M vanish at both rest positions, but their ratio doesn't, as both are linear in x for small displacements. However, neither is strictly linear, which yields the well-known non-isochronism of the simple pendulum plus, relevant for this experiment, a non-trivial tie between extra gravitational pull and induced frequency shift. So, while it's easy to find frequency and relative shift for small oscillations, as the relative extra acceleration can then be considered constant over the swing, non-trivial calculations are necessary for wider swings. In the small oscillation limit it is $2y_M = a_M/a_g$ at first order, as it can be promptly seen. A quick analysis of the arrangements shown in figure 7, with two equal active masses symmetrically placed on either side of the bob, yields for the effect of the two masses on one pendulum

$$\omega_M = \omega_p(1+y_M) = \sqrt{\frac{g}{L}}\left(1+\frac{\rho_M}{\rho_E}\frac{L}{R_E}\left(\frac{R}{a}\right)^3\Gamma(0)\right), \qquad (13)$$

where $\Gamma(0)$ is the value taken at x=0 by the geometrical factor function $\Gamma(x)$, which depends on shape and positioning of the active masses system. In equation (13) ρ_M and ρ_E are the densities of active masses and Earth respectively, and R_E is the Earth's radius, L depends on the pendulum that is considered, being L_f for the fast and L_s for the slow one, and R and a are defined in figure 7. For spheres $\Gamma_{sph}(0)=1$ and for cylinders $\Gamma_{cyl}(0)=(a/R)a^2w/\{\frac{2}{3}(a^2+w^2)^{3/2}\}$, which comes to the value $3/(4\sqrt{2})$, or roughly ½, if $a \approx w \approx R$.

For wider oscillations the shift can't be figured out so easily as in equation (13) because the relative extra acceleration depends on x, which imposes a non-trivial integration in extracting a G determination from frequency shift data. In order to minimize the impact of this fact on uncertainty, the choice is made here to opt for cylindrical masses because of the considerably higher uniformity of $\Gamma_{cyl}(x)$ as compared with $\Gamma_{sph}(x)$ of the spherical ones. Both geometrical factor functions are responsible for the shape of curves shown in figure 8, and the rationality of the choice appears obvious when considering that Q maximization imposes for the swing amplitude θ_0 values of the order of those highlighted in the figure. The signal size price of choosing cylinders may appear steep in view of the already tiny effect, but the gain in accuracy of G value extraction is so great that it's judged to offset it more than adequately.

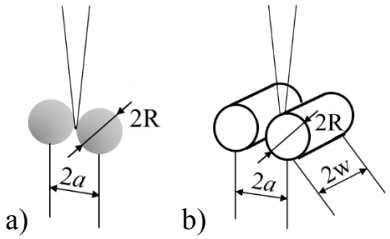

Figure 7. Experimental arrangements for spherical and cylindrical active masses. The bob swings in the centre of the gap between masses.

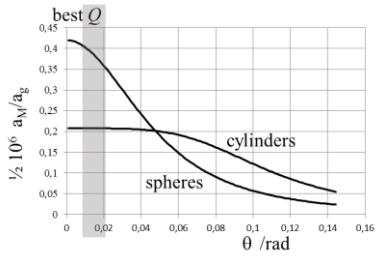

Figure 8. Profile versus θ of the ratio a_M/a_g for a 1 m long pendulum. Tungsten active masses are assumed, with R=50 mm and w/a=1.25.

Full expressions of $\Gamma(x)$ used in figure 8 for both cases, written with $\eta = w/a$ and $\xi = x/a$, are

$$\Gamma_{sph}(x) = (1+\xi^2)^{-3/2}, \qquad (14)$$

$$\Gamma_{cyl}(x) = \frac{3}{4}\frac{a}{R\xi}\left(\frac{1}{\sqrt{1+(\eta-\xi)^2}}-\frac{1}{\sqrt{1+(\eta+\xi)^2}}\right), \qquad (15)$$

Equation (15) was used as a basis to calculate the local acceleration profile shown in figure 4 for the case of seven twin cylindrical active masses. In that case, the reported acceleration is calculated as a function of the rest position of the bob, with the aim of illustrating how the frequency shift is symmetric around zero when the system of masses is moved by the separation between pendulums. In fact, it can be easily seen that an infinite periodic structure of active masses would yield a perfectly periodic and symmetric function of position. It turns out (see figures 9 and 10 below) that the system of seven pairs shown in figure 3 is enough to keep well below 10^{-4} the relative acceleration variation around the rest positions of the two pendulums, up to peak swing amplitudes suitable for Q maximization.

4. Accuracy budget

The formula by which the value of the Newtonian constant G can be extracted from the measured value of Δs as illustrated above can be derived by inverting equation (13). For a single pair of cylinders is

$$G = \frac{\pi \Delta s}{\rho_M \left(T_f^2 + T_s^2\right)} \frac{R}{w} \left[\left(\frac{a}{R}\right)^2 + \left(\frac{w}{R}\right)^2 \right]^{3/2} \qquad (16)$$

Periods T_f and T_s in equation (16) are the small oscillation values for fast and slow pendulums, and must be derived from measured periods by taking into account non-isochronism. However, the correction can be made very accurately if the sweet locally isochronous spot of the minimum in the period versus oscillation amplitude curve is chosen as an operation point, because the mathematical model can provide in this case an adequately accurate prediction of the error [18]. To better than 0.1% the relative value of such error turns out to be $-1.8 \cdot 10^{-5}$ for our 1 m pendulums if D_b = 20 mm (see figure 1), and it occurs at θ_0= 0.017 rad. It appears safe to assume that its contribution to G accuracy may smaller than 10^{-7}.

For the planned seven mass pairs of figure 3 the inversion formula is more complicated because the geometrical factor must take into account all seven contributions. This is not hard for the symmetric positioning, with the bob at the center of the system, but more complex when it turns asymmetric with the bob laying at gap center. Uniformity can be trimmed in both locations by careful design of the cylindrical mass pairs' shape factor $\eta = w/a$. Numerical results for uniformity at the two bob positions are shown for the seven twin masses case in figures 9 and 10. Mass pairs with shape factor η = 1.264 and length $2w$ = 100 mm are assumed, 72 mm in diameter and spaced by 7 mm to host the 5 mm bob and thin vessel walls. Given the uniformity shown for this geometry, it appears reasonable to believe that the integration necessary for connecting G to Δs may be feasible with few percent accuracy, leading to a contribution to accuracy below 10^{-6}. Most of the burden is then left to geometrical accuracy.

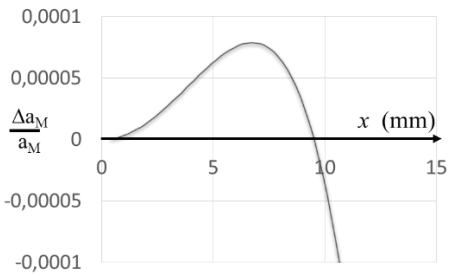

Figure 9. Relative effect at system center from seven twin active masses. Reference for both distance and acceleration is at system center.

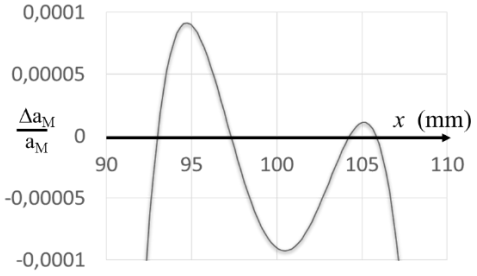

Figure 10. Relative effect at first gap center from seven twin active masses. Distance reference is at system center; acceleration at gap center.

Accuracy on geometry of the active masses system sets the limit for the experiment. In fact, differentiation of the geometrical factor function in equation (16) yields for length and diameter of the active masses a severe constraint of less than 0.5 μm for an accuracy contribution of $6 \cdot 10^{-6}$ on G. However, given the high accuracy of mass measurements, this condition may be relaxed if R is trimmed to reach a given mass (about 7.9 kg for the described Tungsten masses) after cylinders are cut to length, because the bias imposed on the radius will then be $\Delta R/R = -\Delta w/2w$, where Δw is the unknown length error, and the resulting G bias then indicates the less severe constraint of 1 μm for length uncertainty.

Unfortunately, no such compensation can be done on the spacing between the twin cylinders, and the sensitivity calculation then yields for it a harder requirement of 400 nm uncertainty for $6 \cdot 10^{-6}$ on G.

Temperature sensitivity of active masses system geometry is also an issue, as their indicated necessary dimensional accuracy is of the order of 10^{-5}, which requires the non-trivial temperature accuracy and stability of 2 K for the Tungsten masses. No particular problem is instead foreseen for the spacing because of its smaller dimension, which allows a temperature tolerance of about 10 K.

More benign is the requirement on positioning of the bob's trajectory with respect to active masses. In fact it turns out that both in the horizontal and vertical direction the extra acceleration features an extreme versus trajectory positioning, as shown in figure 11 and figure 12 respectively: a minimum in the center for the lateral direction, and a maximum a little above masses' gravity centers for the vertical. The vertical displacement of the maximum is due to the vertical pull down that active masses exert if they are lower than the bob, which adds to Earth's gravity and hence to recall force. For cylinders, such maximum is $(a^2+w^2)/3L$ above the masses' gravity centers (more than 2 mm for the planned size), and the relative shift is below $7\cdot10^{-4}$, which imposes an easy 50 μm tolerance to active masses geometry for a 10^{-6} accuracy contribution from uncertainty on its value. Also, trajectory position tolerance for a safe $2\cdot10^{-6}$ uncertainty contribution is ±0.1 mm in both directions for cylinders of the planned size, just a bit wider than what would be needed for the spheres vertically, but more than three times horizontally.

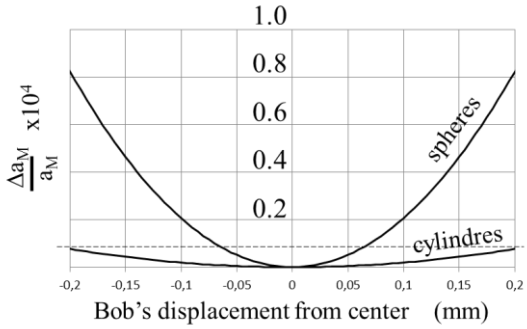

Figure 11. Relative variation of extra pull for lateral displacement of the bob's trajectory from active masses symmetry plane. The dashed line sets bob centering tolerance for 10^{-5} accuracy.

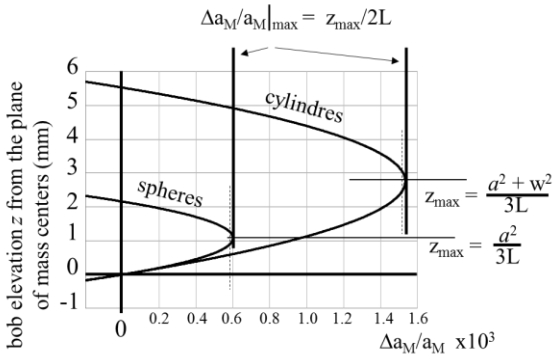

Figure 12. Relative variation of the relevant effect for vertical displacements of the bob's trajectory from the plane of mass centers. Position tolerance for 10^{-5} accuracy is marked by dashed lines.

A summary of the accuracy discussion spelled out here is given in Table 1. It appears that only geometrical uncertainties are expected to be relevant at the level of 10^{-5}, which ushers the possibility of doing even better if resources were to become available to improve geometrical accuracy.

Table 1. Accuracy budget projection based on 1 m long 7.5 μm Carbon fibres, 20 mm diameter suspension profiles, a swing amplitude of 0.017 rad, and a 160 mg bob. Density uniformity is assumed adequate to guarantee positioning uncertainty of the mass center of active masses smaller than 300 nm. For relaxation of dimensional accuracy demand, the diameter of active masses is assumed to be trimmed for accurate mass once the 2*w* length is realized to match the distance between pendulums.

Effect	Relative bias	Uncertainty	conditions
θ dependence of a_M	$<3\cdot10^{-5}$	$<10^{-6}$	Optimization of w/*a*
Shift at bob's vertical position	$6.7\cdot10^{-4}$	$<10^{-6}$	< 50 μm uncertainty in *a* , w
bob's vertical position	0	$2\cdot10^{-6}$	0.2 mm full interval tolerance
bob's lateral position	0	$1.7\cdot10^{-6}$	0.2 mm full interval tolerance
Adiabaticity	$<-2.5\cdot10^{-5}$	$2\cdot10^{-6}$	0.017 rad swing amplitude [11]
Non-isochronism	$-1.8\cdot10^{-5}$	$< 10^{-7}$	Operation at minimum of period
Spacing between twin masses	0	$6\cdot10^{-6}$	0.4 μm gap uncertainty
Active masses dimensions	0	$6\cdot10^{-6}$	0.9 μm uncertainty with mass trimming
Active masses density	0	$5\cdot10^{-6}$	
Total Type B		$1\cdot10^{-5}$	$(\Sigma u_i^2)^{1/2}$
Total Type A		$< 3\cdot10^{-7}$	In three months (based on $3\cdot10^{-6}$ in 1 d)

5. Conclusions

A new experiment was presented for the determination of the Newtonian constant, which is based on a Time and Frequency Metrology approach consisting in the measurement of the small frequency difference between two freely oscillating pendulums via their time delay rate of change. A system of dense active masses is moved back and forth between the two, alternately increasing one frequency and reducing the other, and vice-versa. The increase in resolution by averaging is fast in this case because the limiting noise is white delay noise, which yields $\sigma_y(\tau)$ proportional to $\tau^{-3/2}$. This fact is unique among experiments for the determination of *G*, and offsets the poor signal size problem allowing to focus the design on accuracy rather than S/N ratio. A preliminary experiment is in progress to confirm the possibility, indicated by the analysis, of obtaining *Q* values in the 10^8 range for the pendulums in vacuum, and the construction of the dual pendulum experiment is under way. It is expected that an accuracy of 10^{-5} may be obtained for *G* with the proposed approach, and that it may be possible in a metrology laboratory to reduce limiting geometrical uncertainties enough to push it into the 10^{-6} range.

Acknowledgments
The author wishes to acknowledge the encouragement of many colleagues both over the years and recently in this revisited proposal. In particular should be mentioned Robert Drullinger, Stefan Schlamminger and Bill Phillips of NIST, and Valter Giaretto, Rosario Ceravolo and Lamberto Rondoni of the Politecnico di Torino. The author also wishes to acknowledge the support of the US Department of Commerce and NIST through the Precision Measurements Grant Program. Award ID number 70NANB15H348.

[1] Cavendish H 1798 *Philos. Trans. R. Soc. London* **88** 469
[2] Michaelis W, Haars H and Augustin R 1996 *Metrologia* **32** 267
[3] Kuroda K 1995 *Phys. Rev. Lett.* **75** 2796
[4] Schlamminger S, Holzschuh E, Kundig W, Nolting F, Pixley R E, Schurr J and Straumann U 2006 *Phys. Rev. D* **74** 082001
[5] Schwarz J P, Robertson D S, Niebauer T M and Faller J E 1998 *Science* **282** 2230
[6] Fixler J B, Foster G T, McGuirk J M, Kasevich M A 2007 *Science* **315** 74
[7] Lamporesi G, Bertoldi A, Cacciapuoti L, Prevedelli M and Tino G M 2008 *Phys. Rev. Lett.* **100** 050801
[8] Kleinvoss U, Meyer H, Schumacher A and Hartmann S 1999 *Meas. Sci. Technol.* **10** 492
[9] Parks H V and Faller J E 2010 *Phys. Rev. Lett.* **105** 110801
[10] De Marchi A, Ortolano M, Berutto M and Periale F 2002 *Proc. 6th Symposium on Frequency Standards and Metrology (Fife, Scotland, 10-14 September 2001)* p 538
[11] Berutto M, Ortolano M and De Marchi A 2009 *Metrologia* **46** 119
[12] Gundlach J and Merkowitz M 2000 *Phys. Rev. Lett.* **85** 2869
[13] Armstrong T R and Fitzgerald M P 2003 *Phys. Rev. Lett.* **91** 201101
[14] Quinn T J, Speake C C, Richman S J, Davis R S and Picard A 2001 *Phys. Rev. Lett.* **87** 111101
[15] Luo J, Liu Q, Tu L C, Shao C G, Liu L X, Li S Q, Yang Q and Zhang Y T 2009 *Phys.Rev.Lett.* **102**, 240801
[16] Sullivan D, Allan D, Howe D and Walls F L 1990 *Characterization of clocks and oscillators,* NIST Technical note 1337
[17] Berger J, Davis P and Ekstroem G 2004 *J. Geophys. Res.* **109,** B11307
[18] Maffioli L, 2016 *Mathemetical modelization and experimental validation of a simple pendulum for the measurement of the Newtonian constant G,* Tesi di Laurea, Politecnico di Torino
[19] Ceravolo R, DeMarchi A, Pinotti E, Surace C and Zanotti Fragonara L 2016 *Exp.Mech.* in print
[20] Kurokawa K 1973 *Proc. of IEEE* **61**, 1386
[21] Razavi B 2004 *IEEE J. Sol. State Circ*. **39**, 1415